

Synthesis, Spectroscopic Studies, and Crystal Structures of Phenylorganotin Derivatives with [Bis(2,6-dimethylphenyl)amino]benzoic Acid: Novel Antituberculosis Agents

by Vaso Dokorou^a), Dimitra Kovala-Demertzi*^a), Jerry P. Jasinski^b), Angeliki Galani^a), and Mavroudis A. Demertzis^a)

^a) Inorganic and Analytical Chemistry, Department of Chemistry, University of Ioannina, 45110 Ioannina, Greece (phone: +30-651-98425; fax: +30-651-98792; e-mail: dkovala@cc.uoi.gr)

^b) Department of Chemistry, Keene State College, 229 Main Street, Keene, NH 03435-2110, USA

The novel triphenyl adduct of 2-[(2,6-dimethylphenyl)amino]benzoic acid (HDMPA; **1**), *i.e.*, [SnPh₃(DMPA)] (**2**), the dimeric tetraorganostannoxane [Ph₂(DMPA)SnOSn(DMPA)Ph₂]₂ (**3**), and the monomeric adduct [SnPh₂(DMPA)₂] (**4**), where DMPA is monodeprotonated HDMPA, have been prepared and structurally characterized by means of IR, ¹H-NMR, and ¹³C-NMR spectroscopy. The structures of **1** and **2** have been determined by X-ray crystallography. Single-crystal X-ray-diffraction analysis of **1** revealed that there are two molecules in the asymmetric unit, **HD1** and **HD2**, differing in conformation, both forming centrosymmetric dimers linked by H-bonds between the carboxylic O-atoms. X-Ray analysis of **2** revealed a pentacoordinate structure containing Ph₃Sn coordinated to the carboxylato group. Significant C–H/ π interactions and intramolecular H-bonds stabilize the structures of **1** and **2**, which self-assembled *via* C–H/ π and π / π -stacking interactions. The Ph₃Sn adduct **2** was found to be a promising antimycobacterial lead compound, displaying activity against *Mycobacterium tuberculosis* H37Rv. The cytotoxicity in the Vero cell line is also reported.

Introduction. – 2-[(2,6-Dimethylphenyl)amino]benzoic acid (HDMPA; **1**) resembles *mefenamic acid* (=2-[(2,3-dimethylphenyl)amino]benzoic acid), *tolfenamic acid* (=2-[(3-chloro-2-methylphenyl)amino]benzoic acid), and *flufenamic acid* (=2-[[3-(trifluoromethyl)phenyl]amino]benzoic acid), as well as other commercial fenamates in clinical use. HDMPA was found to inhibit triiodothyronine (T₃) uptake by H4 hepatocytes, and its octanol/H₂O partition coefficient was found to be 5.337 [1]. The anti-inflammatory activity of HDMPA and its derivatives was measured by the anti-UV-erythema test, and the minimum effective dose (*MED*) was found to be 50 mg/kg [2]. The crystal structures of the complexes [Bu₂(DMPA)SnOSn(DMPA)Bu₂]₂ and [Bu₂Sn(DMPA)₂] have been reported [3].

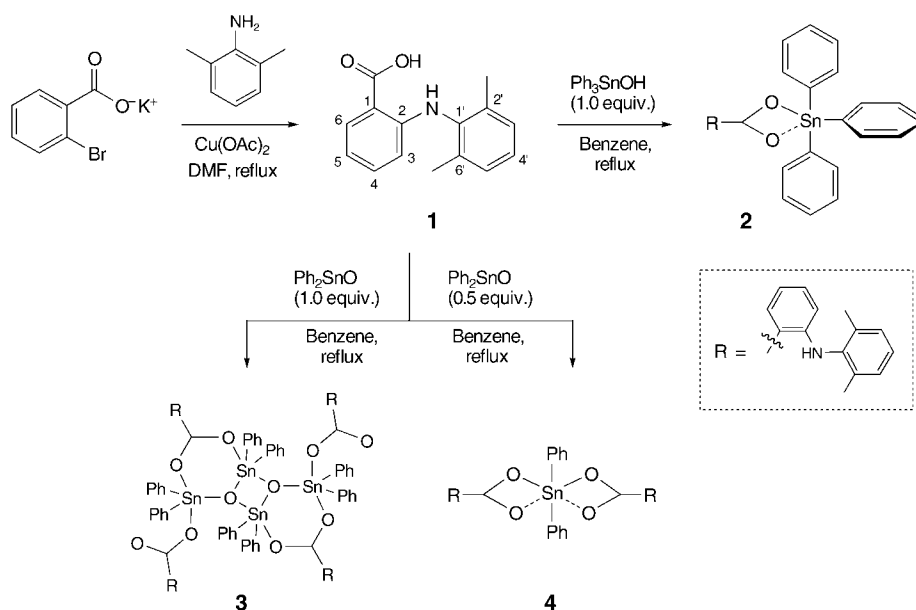
Organotin(IV) carboxylates are an important class of compounds. They are often used as catalysts and stabilizers, biocides, antifouling agents, and wood preservatives [4]. Information on the structures of organotin carboxylates continues to accumulate, and, at the same time, new applications of such compounds are discovered that are relevant for industrial, ecological, and medicinal applications. In recent years, investigations have been carried out to test the antitumour activities of organotin(IV) carboxylates. Several di- and triorganotin species have shown potential as antineoplastic agents [4–7]. In general, triorganotin compounds display a higher biological

activity than their di- and mono-organotin analogues. This has been attributed to their ability to bind to proteins.

As a continuation of our studies on organotin species [8][9], we were interested in the chemistry of organotin/HDMPA compounds and on the coordination chemistry of nonsteroidal anti-inflammatory drugs of the phenylanthranilic acid type, such as *diclofenac* (= [2-[(2,6-dichlorophenyl)amino]phenyl]acetic acid), *mefenamic acid*, and *tolfenamic acid* [10–12]. We, thus, prepared and characterized the novel complexes [SnPh₃(DMPA)] (**2**), the dimeric tetraorganostannoxane [Ph₂(DMPA)SnOSn(DMPA)Ph₂]₂ (**3**), and the diphenyl adduct [SnPh₂(DMPA)₂] (**4**)¹.

Results and Discussion. – *Synthetic Aspects.* Compound **1** was synthesized according to *Ullmann–Goldberg* condensation from 2,6-dimethylaniline and potassium 2-bromobenzoate in the presence of 4-ethylmorpholine and Cu(OAc)₂. Adducts **2**, **3** and **4** were obtained, under azeotropic removal of H₂O, by the reaction of **1** with Ph₃SnOH or Ph₂SnO in a molar ratio of 1:1 for both **2** and **3**, or in a ratio of 2:1 for **3**, respectively (*Scheme*).

Scheme. *Synthesis of Compounds 1–4*



Crystallographic Studies. We were able to obtain single-crystals of **1** and **2** and to solve their structures by X-ray crystallography. Selected interatomic parameters are collected in *Table 1*. Single-crystal X-ray-diffraction analysis of HDMPA (**1**) revealed that there are two molecules in the asymmetric unit, **HD1** and **HD2**, differing in conformation. Both form centrosymmetric dimers linked by H-bonds between the carboxylic O-atoms, as frequently observed for carboxylic acids (*Fig. 1*). The geometry

¹) DMPA represents deprotonated HDMPA (**1**).

of the H-bonds is basically identical in both HDMPA modifications, O(1A)⋯O(2A) being 2.67 Å in **HD1**, and O(1B)⋯O(2B) being 2.66 Å in **HD2**. The NH group is located in a sterically hindered position and, in contrast to *diclofenac* [13], does not participate in an intermolecular H-bond. Both conformers of HDMPA are stabilized by an intramolecular N(1)⋯O(2) H-bond of 2.70- and 2.72-Å length for **HD1** and **HD2**, respectively.

Table 1. Selected Bond Lengths (Å) and Angles (°) for **1** and **2**

1		2	
O(1A)–C(7A)	1.340(14)	Sn(1)–O(1)	2.061(6)
O(2A)–C(7A)	1.241(15)	Sn(1)–O(2)	2.626(7)
O(1B)–C(7B)	1.290(15)	Sn(1)–C(22)	2.110(10)
O(2B)–C(7B)	1.222(15)	Sn(1)–C(16)	2.115(9)
N(1A)–C(2A)	1.363(14)	Sn(1)–C(28)	2.121(9)
N(1A)–C(8A)	1.465(14)	O(1)–C(1)	1.310(10)
N(1B)–C(2B)	1.380(14)	O(2)–C(1)	1.242(10)
N(1B)–C(8B)	1.432(15)	N(1)–C(7)	1.385(11)
		N(1)–C(8)	1.408(11)
C(2A)–N(1A)–C(8A)	122.1(9)	O(1)–Sn(1)–C(22)	110.5(3)
C(2B)–N(1B)–C(8B)	119.9(9)	O(1)–Sn(1)–C(16)	109.3(3)
N(1A)–C(2A)–C(1A)	122.3(10)	C(22)–Sn(1)–C(16)	120.6(4)
N(1A)–C(2A)–C(3A)	120.3(10)	O(1)–Sn(1)–C(28)	96.7(3)
O(1A)–C(7A)–C(1A)	115.4(10)	C(22)–Sn(1)–C(28)	108.4(3)
O(2A)–C(7A)–C(1A)	124.2(11)	O(2)–Sn(1)–C(16)	84.4(3)
O(1A)–C(7A)–O(2A)	120.3(11)	O(2)–Sn(1)–C(28)	150.7(3)
N(1A)–C(8A)–C(13A)	120.6(10)	O(2)–Sn(1)–C(22)	85.2(3)
N(1A)–C(8A)–C(9A)	115.7(10)	O(2)–Sn(1)–O(1)	54.0(2)
		C(16)–Sn(1)–C(28)	108.7(3)
		C(1)–O(1)–Sn(1)	106.4(5)
		C(7)–N(1)–C(8)	124.8(7)
		C(27)–C(22)–Sn(1)	122.8(8)
		C(23)–C(22)–Sn(1)	120.8(7)
		C(33)–C(28)–Sn(1)	123.5(7)
		C(29)–C(28)–Sn(1)	119.2(7)

A significant difference between **HD1** and **HD2** is the geometry of the amino group. In **HD1**, the two N(1)–C bonds are markedly different compared with the more-similar distances in **HD2** ($\Delta d = 0.1$ vs. 0.05 Å for **HD1** and **HD2**, resp.). The C(2)–N(1)–C(8) angle is 122.1° and 119.9° in **HD1** and **HD2**, respectively. In *meclofenamic acid* ($=2$ -[(2,6-dichloro-3-methylphenyl)amino]benzoic acid), with two perpendicular phenyl groups [14a], the C–N–C angle is 123° , and in *niflumic acid* ($=2$ -[[3-(trifluoromethyl)phenyl]amino]pyridine-3-carboxylic acid), where the two phenyl rings are almost coplanar [14b], it is 131° . In the structure of *tolfenamic acid*, the angle is 124.3° for the white form, and 129.0° for the yellow form [15a].

HD1 and **HD2** also differ significantly in the geometry of the COOH group, the largest differences occurring in the C–O bond lengths. More-effective π -electron delocalization is observed in the COOH group of **HD2** [O(1B)–C(7B) 1.290(15) and O(2B)–C(7B) 1.222(15) Å] relative to **HD1** [O(1A)–C(7A) 1.34 and O(2A)–C(7A) 1.24 Å]. The interplanar angle between the two aromatic rings is 88.2 vs. 86.7° for **HD1** and **HD2**, respectively.

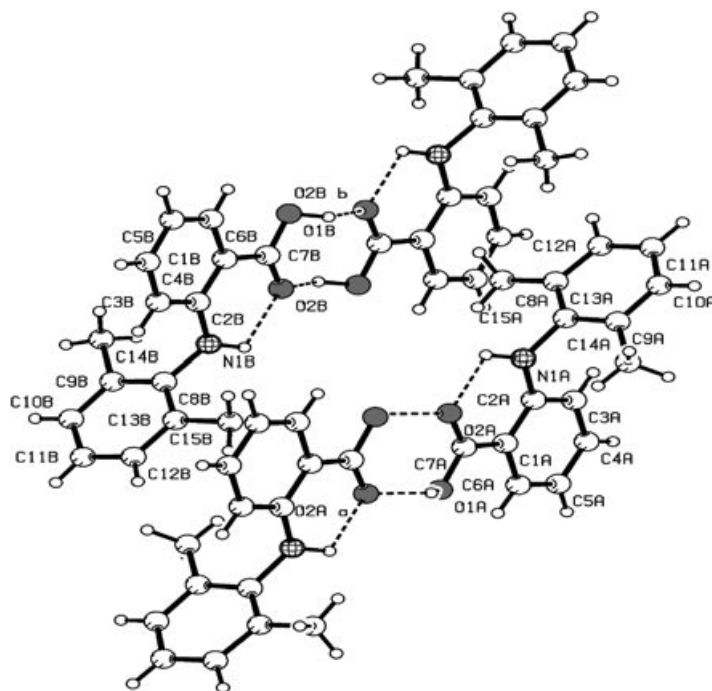


Fig. 1. X-Ray crystal structure of the dimers **HD1** and **HD2** of compound **1**

Flufenamic acid [15b], *tolfenamic acid* [14a], and *diclofenac* [13] have also been isolated in two different crystal forms, respectively. The angles between the two phenyl rings are 53 and 43° in the two conformers of *flufenamic acid* [15b]. In *tolfenamic acid*, the interplanar angle is 73° for the white form and 46° for the yellow form [15a]. In *niflumic acid* [14b], the two rings are almost coplanar, with an angle of 9°, whereas in *meclofenamic acid*, the two planes are virtually perpendicular, the corresponding angle being 81° [14a]. It seems obvious that the conformation of the molecules is determined by steric interactions between the substituents on the phenyl groups. Adjacent to the amino group in *meclofenamic acid* and HDMPA, there are two equivalent Cl-atoms and two Me groups, respectively, and the molecules are in a conformation where the two phenyl rings are almost perpendicular to minimize steric interactions.

The crystallographically determined molecular structure of **2** is shown in Fig. 2. It comprises discrete molecular units in which the COO group functions as an anisobidentate chelating ligand [Sn⋯O(1) 2.06 Å, Sn⋯O(2) 2.62 Å], thus rendering the Sn-atom five-coordinated. The Sn⋯O(2) distance, 2.626(7) Å, is fairly long for an intramolecularly five-coordinated Sn-atom, and indicates significant bonding interactions. However, Sn⋯O distances of 2.61–3.02 Å have been reported for such intramolecular bonds [16]. The intramolecular H-bond formed from the amino group [O(2)⋯N(1) 2.68 Å] contributes to an elongated Sn–O(2) bond. A similar H-bonded situation was found in the *mefenamic acid* adduct [Ph₃Sn[(mef)] [7].

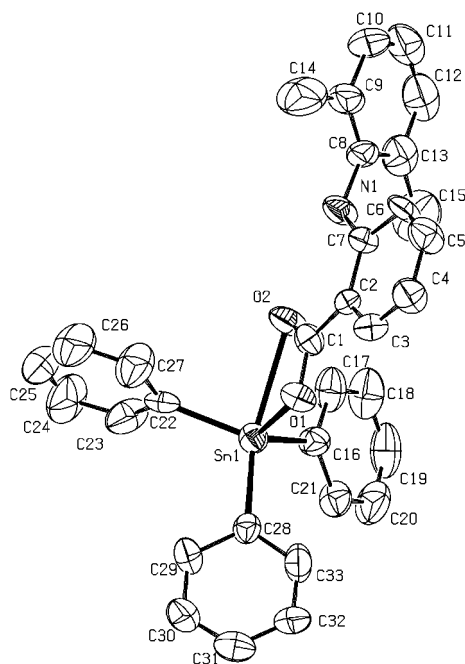
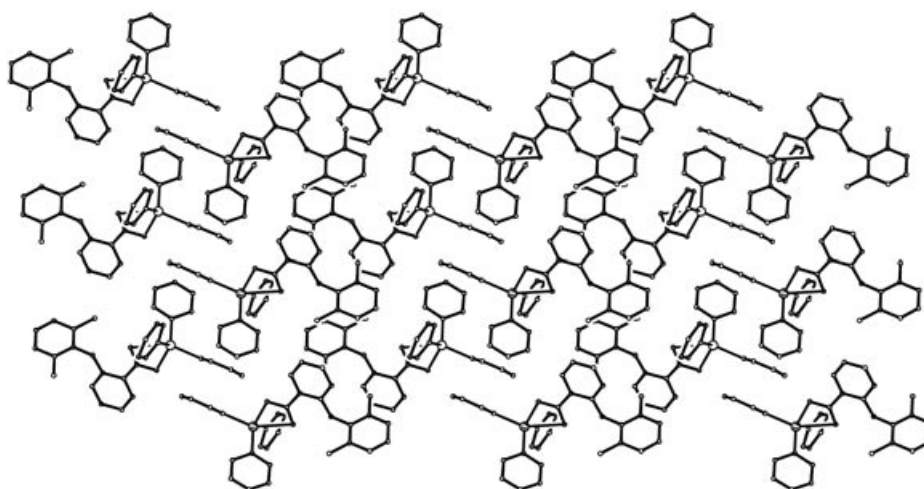


Fig. 2. X-Ray crystal structure of **2**

Analysis of the shape-determining angles of **2** using the approach of *Reedijk* and co-workers [17] yields a $\tau(\alpha - \beta)/60$ value of 0.66 for Sn ($\tau = 0$ and 1 for *sp* and *tbp* geometries, resp.). The geometry at the Sn-atom is represented by a distorted *cis*-trigonal bipyramid in which the carboxylato ligand spans equatorial and axial sites. The two C–O bond distances of the C=O group are unequal [1.31 vs. 1.24 Å], the longer C–O distance being associated with the shorter Sn–O bond, and *vice versa*.

The structures of a number of triorganotin carboxylates have been determined by X-ray diffraction [18–20]. In the crystalline state, these compounds generally adopt either a polymeric structure with a five-coordinated Sn-atom, or a discrete five-coordinated form. A polymeric structure for triphenyl carboxylates is associated with the R' group, R'COO[−] being electron-withdrawing. A delicate energy balance plays between these two forms, although the electronegativity of the phenyl group has been cited as a factor influencing the formation of the discrete form, since it gives more access to an axial position of a trigonal bipyramid [19][20]. The axial Sn-ligand bond lengths in both forms are subject to variations that depend on substituents, electronegativity, ring strain, H-bonds, and steric interactions [21]. The phenyl rings in **2** are planar. The dihedral angle between the planes of the phenyl rings of DMPA in **2** is 68.6°, while, for **HD1** and **HD2**, it is 88.2 and 86.7°, respectively. The crystal structure of **2** shows C–H/ π interactions and intramolecular H-bonds. The polar amino H-atom participates in an intramolecular H-bond (*Table 2*). Complex **2** self-assembles *via* C–H/ π and weak π/π stacking interactions (*Fig. 3*).

Fig. 3. Crystal-structure packing of **2** viewed along the *a*-axis of the unit cellTable 2. *C–H/π Interactions and Intramolecular H-Bonds and Distances (···) for Compounds 1 and 2. Distances in Å, angles in degrees (°); X is a C-, O-, or N-atom, Z is either a centroid (Cg) or an O-atom. See Figs 1 and 2 for atom numbering.*

X	H	Z	H···Z	X···Z	∠(X–H···Z)
C–H/π (1)					
C(14A)	H(3)	Cg(1) ^{a)}	2.75	3.54	141.6
C(14B)	H(12)	Cg(2) ^{a)}	2.75	3.57	134.0
H-bonds (1)					
O(1B) ^{b)}	H(31)	O(2B)	1.89	2.67	138
O(1A)	H(34)	O(2A)	1.83	2.66	140
N(1A)	H(14)	O(2A)	2.07	2.70	121
N(1B)	H(13)	O(2B)	2.14	2.72	120
C–H/π (2)					
C(5)	H(3)	Cg(3) ^{c)} ^{d)}	2.78	3.58	142.0
C(30)	H(8)	Cg(4) ^{e)}	2.99	3.65	127.9
C(19)	H(16)	Cg(5) ^{f)}	3.20	3.79	121.3
C(23)	H(21)	Cg(5) ^{e)}	2.94	3.82	155.3
C(15)	H(24)	Cg(3) ^{g)}	3.28	3.96	129.6
H-bond (2)					
N(1)	H(29)	O(2)	1.98	2.69	128

^{a)} Cg(1) and Cg(2) refer to the centroids C(9B)···C(13B) and C(9A)···C(13A), resp.; symmetry: $x, 1+y, -1+z$. ^{b)} Symmetry: $-x, -y, 1-z$. ^{c)} Cg(3) to Cg(5) refer to the centroids C(8)···C(13), C(16)···C(21), and C(28)···C(33), resp. ^{d)} Symmetry: $3-x, -y, 3-z$. ^{e)} Symmetry: $1-x, -1-y, 2-z$. ^{f)} Symmetry: $x, y, -1+z$. ^{g)} Symmetry: $2-x, -y, 2-z$.

Spectroscopic Studies. In the IR spectrum of HDMPA (**1**), the strong band at 3340 cm^{-1} was assigned to the N–H stretching motion, and the broad band at *ca.* 2980 cm^{-1} to the $\nu(\text{NH}\cdots\text{O})$ and $\nu(\text{OH}\cdots\text{O})$ mode due to intra- and intermolecular H-bonding [7][22], as confirmed by X-ray crystallography. The absence of large systematic shifts of the $\nu(\text{NH})$ and $\delta(\text{NH})$ bands in the spectra of the complexes

compared with those of the ligand indicates that there is no interaction between the NH group and the metal ions. The $\nu_{\text{asym}}(\text{COO})$ and $\nu_{\text{sym}}(\text{COO})$ bands appear at *ca.* 1650–1570 and 1450–1390 cm^{-1} , respectively. The $\nu_{\text{asym}}(\text{COO})$ and $\nu_{\text{sym}}(\text{COO})$ bands appear at 1654 and 1396 cm^{-1} for **2**, and at 1615 and 1361 cm^{-1} for $[\text{SnPh}_2(\text{DMPA})_2]$ (**4**). The difference $\nu_{\text{asym}}(\text{COO}) - \nu_{\text{sym}}(\text{COO})$ between these frequencies is 254 and 258 cm^{-1} , respectively, for **2** and **4**, which is close to that found for the anisobidentate carboxylato group [3]. The $\nu_{\text{asym}}(\text{COO})$ and $\nu_{\text{sym}}(\text{COO})$ bands appear at 1615 and 1576 cm^{-1} , and at 1394 and 1453 cm^{-1} , respectively, for **3**. The $\nu_{\text{asym}}(\text{COO}) - \nu_{\text{sym}}(\text{COO})$ value between these frequencies for **3** is close to that found for monodentate (221 cm^{-1}) and bridging bidentate carboxylato groups (123 cm^{-1}). A very strong band near 600 cm^{-1} for **3** is characteristic of the Sn–O–Sn linkage. Two bands at 600–620 cm^{-1} for **3** are assigned to symmetric and asymmetric $(\text{SnO})_2$ vibrations, indicating nonlinear O–Sn–O moieties. The bands at 320–280 cm^{-1} are assigned to the Sn–O (COO) stretching modes. The absorption bands at 360–340 cm^{-1} are attributed to $\nu(\text{Sn}-\text{C})$ stretching modes [3][7][22].

The ^1H - and ^{13}C -NMR chemical shifts of both the ligand and the complexes were recorded in CDCl_3 solution. The downfield chemical shift for NH in the ^1H -NMR spectrum of the ligand indicates that this H-atom is involved in H-bonding. The crystal structure of HDMPA (**1**) shows the presence of an intramolecular H-bond between the NH group and the carbonyl O-atom of the COO group. In the complexes **2–4**, H–C(3) is deshielded due to σ -charge donation from the COO^- donor to the Sn center, which reduces the electron density at the ligand. The observed upfield shift for both H–C(4) and C(4) *para* to the coordinating COO group could be due to a backflow of charge from the Sn-atom to the aromatic ring [7][9][23].

The involvement of the COO group in bonding to Sn was confirmed by the $\delta(\text{C}(1))$ and $\delta(\text{C}(6))$ chemical shifts, which were strongly affected upon coordination. The remaining $\delta(\text{C})$ values of the aromatic ring were not significantly shifted on binding. Interestingly, no ^{13}C -NMR resonance attributable to the COO group (C(1)) was observed for the complexes, a behavior that has been noted previously for related systems [7–9].

Biological Activity. Compounds **1** and **2** were tested against *Mycobacterium tuberculosis* H37Rv in BACTEK-12B medium, using the BACTEC 460-radiometric system at the single concentration of 6.25 $\mu\text{g}/\text{ml}$. Compounds **3** and **4** were not soluble in DMSO or H_2O , and were not screened. *Rifampicin* was included as a positive drug control. HDMPA (**1**) did not exhibit any inhibitory effect and was not screened any further. Complex **2** exhibited the highest inhibitory activity (100%) and can be considered an active compound. Generally, compounds that exhibit less than 90% inhibition in the primary screen ($\text{MIC} > 6.25 \mu\text{g}/\text{ml}$)²⁾ were not evaluated further. Compound **2**, effecting $>90\%$ inhibition in the primary screen at 6.25 $\mu\text{g}/\text{ml}$, was tested again at lower concentration against *Mycobacterium tuberculosis* H37Rv to determine the MIC value in a broth-microdilution assay with *Alamar Blue*. The MIC values determined were 0.78 for **2**, 0.39 for $[\text{SnPh}_3(\text{mef})]$, and $>6.25 \mu\text{g}/\text{ml}$ for $[\text{SnBu}_2(\text{mef})_2]$, where ‘mef’ is deprotonated *mefenamic acid* (Table 3) [7].

²⁾ MIC stands for minimum inhibitory concentration.

Table 3. *Biological Activities of Compounds 1 and 2 towards Mycobacterium tuberculosis H37Rv Compared to Selected Reference Compounds. Alamar Blue assay; drug conc. 6.25 µg/ml; for details, see the Exper. Part. The term 'mef' stands for deprotonated mefenamic acid (= 2-[(2,3-dimethylphenyl)amino]benzoic acid).*

Compound	Inhibition (%)	MIC [µg/ml]	IC ₅₀ [µg/ml]
HDMPA (1)	0		
[Sn(Ph) ₃ (DMPA)] (2)	100	0.78	1.89
[SnPh ₃ (mef)] [7]	98	0.39	
[SnBu ₂ (mef) ₂] [7]	92	> 6.25	
Rifampicin ^{a)}	95	0.25	113.6

^{a)} Positive drug control.

Compound **2** was tested for cytotoxicity (IC₅₀) in Vero cells at concentrations equal to and greater than the MIC value for *Mycobacterium tuberculosis* H37Rv. The IC₅₀ value was found to be 1.89 µg/ml for **2**. The selectivity index (SI = IC₅₀/MIC) was calculated as 2.42, showing that this compound not only displays a considerable activity, but also an increased cytotoxicity. The significance of the MIC value depends on several factors such as compound structure, novelty, toxicity, and potential mechanism of action. Generally, an MIC value of ≤ 1 µg/ml for a novel compound is considered an excellent lead.

Conclusions. – Three novel phenyl adducts of 2-[(2,6-dimethylphenyl)amino]benzoic acid (HDMPA; **1**), *i.e.*, [SnPh₃(DMPA)] (**2**), [Ph₂(DMPA)SnOSn(DMPA)Ph₂]₂ (**3**), and [SnPh₂(DMPA)₂] (**4**) have been prepared and structurally characterized by means of IR, ¹H-NMR, and ¹³C-NMR spectroscopy. Based on spectroscopic data, dimeric tetraorganostannoxane and monomeric structures are proposed for **3** and **4**, respectively. The structures of **1** and **2** were determined by X-ray crystallography, showing significant C–H/π interactions and intramolecular H-bonds. The triphenyl adduct **2** and the parent compound **1** were tested for their antimycobacterial activities against *Mycobacterium tuberculosis* H37Rv. Compound **2**, a Ph₃Sn derivative of anthranilic acid, was found to be an excellent lead compound, which makes this novel class of compounds potential new antituberculosis agents.

Experimental Part

General. All reagents were commercially available (*Aldrich* or *Merck*) and used as supplied. Solvents were purified according to standard procedures. Melting points (m.p.) were determined in open capillaries and are uncorrected. IR and far-IR Spectra: *Nicolet 55XC* FT-IR spectrophotometer, KBr pellets (4000–400 cm⁻¹), and nujol mulls dispersed between polyethylene disks (400–40 cm⁻¹). ¹H- and ¹³C-NMR Spectra: *Bruker AMX-400* and *Bruker AC-250* spectrometers; at 250.13 MHz (¹H) and 62.90 MHz (¹³C) in CDCl₃ soln. at r.t.; chemical shifts δ in ppm rel. to residual solvent signal (7.24 ppm). Elemental analyses were carried out by the microanalytical service of the University of Ioannina, Greece.

2-[(2,6-Dimethylphenyl)amino]benzoic Acid (HDMPA; **1**). This compound was synthesized by *Ullmann–Goldberg* condensation [1]. 2,6-Dimethylaniline (5.60 g, 46 mmol), potassium 2-bromobenzoate (11.36 g, 47 mmol), 4-ethylmorpholine (5.46 g, 47 mmole), and anh. Cu(OAc)₂ (0.5 g) in distilled DMF (20 ml) were refluxed for 3 h under N₂ atmosphere. The resulting soln. was treated with DMF (13 ml) and 12% aq. HCl soln. (19 ml). The aq. layer was decanted, and MeOH was added. The solid was collected and recrystallized three times from acetone to afford **1** (2.70 g, 24%). M.p. 209–210°. IR (KBr): 3348 (ν(OH)), 3289, 2980 (ν(NH)), 1610 (ν_{asym}(COO)), 1448 (ν_{sym}(COO)). ¹H-NMR (CDCl₃): 8.90 (s, NH); 8.04 (d, H–C(6));

7.27 (*t*, H–C(4)); 7.15 (*m*, H–C(3',4',5')); 6.66 (*t*, H–C(5)); 6.22 (*d*, H–C(4)); 2.22 (*s*, 2 Me). ^{13}C -NMR: 170.7 (COOH); 156.8 (C(2)); 135.6 (C(4)); 132.5 (C(6)); 116.2 (C(1)); 115.7 (C(5)); 112.7 (C(3)); 18.2 (2 Me). Anal. calc. for $\text{C}_{15}\text{H}_{15}\text{NO}_2$; 241.11 g mol^{-1} ; C 74.76, H 6.27, N 5.81; found: C 73.9, H 6.6, N 5.8. X-Ray single-crystal structure: see Fig. 1 and Tables 1, 2, and 4.

(2-[(2,6-Dimethylphenyl)amino]benzoato)triphenyltin(IV) (**2**). Ph_3SnOH (0.422 g, 1.15 mmol) and **1** (0.241 g, 1.00 mmol) in benzene (40 ml) were refluxed overnight under azeotropic removal of H_2O (Dean–Stark trap). The resulting clear yellow soln. was concentrated *in vacuo* to a small volume, chilled, and triturated with trifluoroacetic acid (TFA) to afford a white-yellow solid. Drops of acetone were added, and, after slow evaporation, compound **2** was isolated by filtration, washed with acetone, and dried *in vacuo* over silica gel. Yield: 0.416 g (70%). White-yellow powder. M.p. 178–180°. IR (KBr): 3298 ($\nu(\text{NH})$), 1615 ($\nu_{\text{asym}}(\text{COO})$), 1361 ($\nu_{\text{sym}}(\text{COO})$), 347 (br., $\nu(\text{Sn–C})$), 323, 283 ($\nu(\text{Sn–O})$), 177, 154 ($\delta(\text{Sn–O})$). ^1H -NMR (CDCl_3): 9.12 (*s*, NH); 8.15 (*d*, H–C(6)); 7.79 (*s*, *o*-H of Ph); 7.39 (*s*, *m*-H of Ph); 7.44 (*s*, *p*-H of Ph); 7.12 (*t*, H–C(4)); 7.12 (*m*, H–C(3',4',5')); 6.62 (*t*, H–C(5)); 6.19 (*d*, H–C(3)); 2.16 (*s*, 2 Me). ^{13}C -NMR: 149.9 (C(2)); 138.9 (*o*-C of Ph); 130.0 (*m*-C of Ph); 134.5 (C(6)); 134.5 (C(4)); 128.8 (*p*-C of Ph); 126.4 (C(1)); 115.5 (C(5)); 112.4 (C(3)), 29.7; 18.3 (2 Me). Anal. calc. for $\text{C}_{33}\text{H}_{29}\text{NO}_2\text{Sn}$ (590.30 g mol^{-1}); C 67.14, H 4.95, N 2.37; found: C 66.81, H 4.99, N 2.40. X-Ray single-crystal structure: see Figs. 2 and 3, and Tables 1, 2, and 4.

1,2:3,4-Di- μ_2 -2-[(2,3-dimethylphenyl)amino]benzoato-O,O-I,3-bis-2-[(2,3-dimethylphenyl)amino]benzoato-O-I,2,4:2,3,4-di- μ_3 -oxo-tetrakis[diphenyltin(IV)] (**3**). Ph_2SnO (0.332 g, 1.15 mmol) and **1** (0.241 g, 1.00 mmol) in benzene (40 ml) were refluxed for 24 h under azeotropic removal of H_2O (Dean–Stark trap). The resulting clear soln. was concentrated *in vacuo* to a small volume. Drops of MeOH were added, and, after slow evaporation, **3** was isolated by filtration, washed with acetone, and dried *in vacuo* over silica gel. Yield: 0.482 g (53%). White powder. M.p. 150–152°. IR (KBr): 3346, 3299 ($\nu(\text{NH})$), 1615 ($\nu_{\text{asym}}(\text{COO})$), 1394 ($\nu_{\text{sym}}(\text{COO})$), 1576 ($\nu_{\text{sym}}(\text{COO})$), 1453 ($\nu_{\text{sym}}(\text{COO})$), 663 ($\nu(\text{Sn–O})_2$), 366, 348, ($\nu(\text{Sn–C})$), 313, 296, 277 ($\nu(\text{Sn–O})$), 148 ($\delta(\text{Sn–O})$). ^1H -NMR (CDCl_3): 8.92 (br., NH); 8.18, 8.08 (*d*, H–C(6)); 7.81 (*s*, *o*-H of Ph), 7.36–7.45 (*m*, *m*-H and *p*-H of Ph); 7.25 (*m*, H–C(3',4',5')); 7.12 (*t*, 5 H); 6.66 (*m*, 4 H); 6.21 (*m*, 6 H); 3.48, 2.18 (2*s*, 8 Me). ^{13}C -NMR: 139.4 (C(2)); 138.9 (*o*-C of Ph); 135.4 (C(4)); 133.5 (C(6)); 130.0 (*m*-C of Ph); 128.5 (*p*-C of Ph); 126.5 (C(1)); 115.6 (C(5)); 112.5 (C(3)); 18.3 (8 Me). Anal. calc. for $\text{C}_{108}\text{H}_{96}\text{N}_4\text{O}_{10}\text{Sn}_4$ (2084.77 g mol^{-1}) C 62.22, H 4.64, N 2.69; found: C 62.18, H 4.23; N 3.15.

(Bis-2-[(2,6-dimethylphenyl)amino]benzoato)diphenyltin(IV) (**4**). Ph_2SnO (0.289 g, 1.00 mmol) and **1** (0.519 g, 2.15 mmol) in benzene (40 ml) were refluxed for 24 h under azeotropic removal of H_2O (Dean–Stark trap). The resulting clear soln. was concentrated *in vacuo* to a small volume. The oily product was dissolved in MeOH. After slow evaporation, **4** was isolated by filtration, washed with acetone, and dried *in vacuo* over silica gel. Yield: 0.550 g (70%). White-yellow powder. M.p. 180–184°. IR (KBr): 3341 ($\nu(\text{NH})$), 1654 ($\nu_{\text{asym}}(\text{COO})$), 1396 ($\nu_{\text{sym}}(\text{COO})$), 364, 352 ($\nu(\text{Sn–C})$), 314, 298 ($\nu(\text{Sn–O})$), 177 ($\delta(\text{Sn–O})$). ^1H -NMR (CDCl_3): 8.88 (br., NH); 8.07 (*d*, H–C(6)), 6.68 (*t*, H–C(5)); 7.13 (*t*, H–C(4)); 6.22 (*d*, H–C(3)); 7.21 (*m*, H–C(3',4',5')); 2.18 (*s*, 8 Me); 7.86 (*s*, *o*-H of Ph); 7.45 (*m*, *m*-H and *p*-H of Ph). ^{13}C -NMR: 150.6 (C(2)); 126.7 (C(1)); 136.8 (C(6)); 115.7 (C(5)); 135.6 (C(4)); 112.7 (C(3)); 136.9 (*o*-C of Ph), 130.0 (*m*-C of Ph), 128.5 (*p*-C of Ph), 27.9, 18.3 (4 Me). Anal. calc. for $\text{C}_{42}\text{H}_{38}\text{N}_2\text{O}_4\text{Sn}$ (753.47 g mol^{-1}); C 66.95, H 5.08, N 3.72; found: C 66.58, H 5.28, N 3.63.

X-Ray Crystallography. The crystallographic data for **1** and **2** are given in Table 4, together with refinement details. All measurements were performed on a Rigaku AFC6S diffractometer, with graphite-monochromated MoK_α radiation. The data were collected in the ω - 2θ mode to a maximum 2θ value of 55.2°. The structures of **1** and **2** were solved by direct methods and expanded by Fourier techniques [24]. The non-H-atoms were refined anisotropically. H-atoms were included, but not refined. All calculations were performed with the teXsan [24] crystallographic software package (Molecular Structure Corporation), except for refinement, which was performed with SHELXL-97 [25]. Crystallographic data for the structural analyses have been deposited with the Cambridge Crystallographic Data Centre, as deposition numbers CCDC-233330 (**1**) and CCDC-233331 (**2**). Copies of these data may be obtained, free of charge, from CCDC, 12 Union Road, Cambridge CB2 1EZ, UK, via fax (+44-1223-336-033), e-mail (deposit@ccdc.cam.ac.uk), or internet (www.ccdc.cam.ac.uk).

Antituberculosis Assay. *In vitro* evaluation of the activity of **1** and **2** against *Mycobacterium tuberculosis* H37Rv was determined with the modified BACTEC-460 system. A screen was conducted at 6.25 $\mu\text{g/ml}$ against *M. tuberculosis* H37Rv in BACTEC-12B medium, using the BACTEC-460 radiometric system. Compounds effecting < 90% inhibition in the primary screen ($\text{MIC} > 6.25 \mu\text{g/ml}$) were not evaluated further. Compounds demonstrating at least 90% inhibition were re-investigated at lower concentration in a broth-microdilution assay with Alamar Blue (MABA). The minimum inhibitory concentration (MIC) was defined as the lowest concentration effecting a reduction in fluorescence of 90% relative to blanks. Rifampicin, used as a positive drug control, was dissolved in DMSO and added to BACTEC-12 broth to achieve a range of concentrations for

Table 4. *X-Ray Crystal Data and Structure Refinement*

	1	2
Crystallized from	THF/acetone	Benzene/EtOH
Crystal size [mm]	0.30 × 0.40 × 0.40	0.30 × 0.30 × 0.50
Formula	C ₁₅ H ₁₅ NO ₂	C ₃₃ H ₂₉ NO ₂ S
<i>M_r</i>	241.28	590.26
<i>T</i> [K]	296(2)	296(2)
<i>λ</i> [Å]	0.71069	0.71069
Crystal system	Triclinic	Triclinic
Space group	<i>P</i> 1̄ (No. 2)	<i>P</i> 1̄ (No. 2)
Cell dimensions:		
<i>a</i> [Å]	15.8375(16)	9.733(8)
<i>b</i> [Å]	7.5311(7)	17.73(1)
<i>c</i> [Å]	11.1845(12)	8.844(6)
<i>α</i> [°]	83.728(9)	90.20(6)
<i>β</i> [°]	104.806(9)	107.38(6)
<i>γ</i> [°]	79.038(8)	105.49(6)
<i>V</i> [Å ³]	1248.6(2)	1398(2)
<i>Z</i>	4	2
<i>D_c</i> [Mg m ⁻³]	1.283	1.402
Absorption coefficient	0.085	0.943
<i>F</i> (000)	512	600
<i>θ</i> Range [°]	1.9 to 27.5	2.26 to 27.58
Ranges of <i>h, k, l</i>	0 ≤ <i>h</i> ≤ 20, -9 ≤ <i>k</i> ≤ 9, 14 ≤ <i>l</i> ≤ 14	0 ≤ <i>h</i> ≤ 12, -23 ≤ <i>k</i> ≤ 22, -1 ≤ <i>l</i> ≤ 10
Refl. collected, unique	5948, 5738	6833 / 6450
<i>R</i> (int)	0.152	0.118
Refinement	Full-matrix least-squares on <i>F</i> ²	Full-matrix least-squares on <i>F</i> ²
Data, restraints, parameters	5738, 0, 325	6450, 0, 334
Goodness-of-fit on <i>F</i> ²	0.83	1.039
Final <i>R</i> ₁ / <i>wR</i> ₂ (<i>I</i> > 2σ(<i>I</i>))	0.0553, 0.3875	0.0597, 0.2179
Largest diff. peak/hole [e Å ⁻³]	-0.28, 0.26	1.012, -1.300

the determination of the *MIC* value, the lowest concentration inhibiting 99% of the inocula. The *MIC* value of *Rifampicin* is 0.25 µg/ml, with 95% inhibition of the H37Rv strain.

Cytotoxicity Assay. Compound **2** was tested for its cytotoxicity (in terms of *IC*₅₀) in Vero cells at concentrations ≤ 6.25 µg/ml, or ten times the *MIC* value for *M. tuberculosis* H37Rv. After 72 h of exposure, viability was assessed on the basis of cellular conversion of MTT into a formazan product, using the *Promega CellTier-96 Nonradiative Cell-Proliferation Assay*. The selectivity index, *SI*, is the ratio of the measured *IC*₅₀ value in Vero cells to the *MIC* value described above. *IC*₅₀ and *SI* Values for controls: *rifampicin*, *IC*₅₀ = 113.6 µg/ml (*SI* > 800); DMSO = 0.0099; DMSO at 1:50 > 1%.

We thank the *European Community* and the *Greek Ministry of Education and Religion* for funding via the *epeak herakleitos* research program. *V. D.* thanks the same authorities for a scholarship. We also thank the NMR service of the University of Ioannina, Greece. We are grateful to Dr. *Cecil D. Kwong* (Tuberculosis Antimicrobial Acquisition & Coordinating Facility (TAACF), National Institute of Allergy and Infectious Diseases Southern Research Institute, GWL Hansen's Disease Center, Colorado State University, Birmingham, Alabama, USA) for the *in vitro* evaluation of antimycobacterial activity.

REFERENCES

- [1] J. S. Kaltenbrom, R. A. Scherrer, F. W. Short, H. R. Beatty, M. M. Saka, C. V. Winder, J. Wax, W. R. N. Williamson, *Arzneim.-Forsch.* **1983**, 33(1), 621.
- [2] D. K. Chalmers, G. H. Scholz, D. J. Topliss, E. Koliniatis, S. L. A. Munro, D. J. Craik, M. Iskander, J. R. Stockigt, *J. Med. Chem.* **1993**, 36, 1272.
- [3] V. Dokorou, M. A. Demertzis, J. P. Jasinski, D. Kovala-Demertzi, *J. Organomet. Chem.* **2004**, 689, 317.
- [4] A. G. Davies, 'Organotin Chemistry', VCH, Weinheim, 1997; 'Chemistry of Tin', 2nd edn., Ed. P. J. Smith, Blackie Academic and Professional, London, 1998.
- [5] M. Gielen, *Appl. Organomet. Chem.* **2002**, 16, 481; M. Gielen, *Coord. Chem. Rev.* **1996**, 15, 41.
- [6] S. J. Blunden, P. A. Cusack, R. Hill, 'Industrial Uses of Tin Chemicals', Royal Society of Chemistry, London, 1985; A. J. Crowe, in 'Metal-Based Antitumour Drugs', Ed. M. Gielen, Freund, London, 1989, Vol. 1.
- [7] D. Kovala-Demertzi, V. Dokorou, Z. Ciunik, N. Kourkoumelis, M. Demertzis, *Appl. Organomet. Chem.* **2002**, 16, 360.
- [8] D. Kovala-Demertzi, P. Tauridou, A. Moukarika, J. M. Tsangaris, C. P. Raptopoulou, A. Terzis, *J. Chem. Soc., Dalton Trans.* **1995**, 123; D. Kovala-Demertzi, P. Tauridou, U. Russo, M. Gielen, *Inorg. Chim. Acta* **1995**, 239, 177; S. K. Hadjikakou, M. A. Demertzis, J. R. Miller, D. Kovala-Demertzi, *J. Chem. Soc., Dalton Trans.* **1999**, 663.
- [9] M. A. Demertzis, S. K. Hadjikakou, D. Kovala-Demertzi, A. Koutsodimou, M. Kubicki, *Helv. Chim. Acta* **2000**, 83, 2787.
- [10] V. Dokorou, Z. Ciunik, U. Russo, D. Kovala-Demertzi, *J. Organomet. Chem.* **2001**, 630, 205.
- [11] D. Kovala-Demertzi, N. Kourkoumelis, A. Koutsodimou, A. Moukarika, E. Horn, E. R. T. Tiekink, *J. Organomet. Chem.* **2001**, 620, 194.
- [12] N. Kourkoumelis, D. Kovala-Demertzi, E. Tiekink, *Z. Crystallogr.* **1999**, 214, 758; N. Kourkoumelis, A. Hatzidimitriou, D. Kovala-Demertzi, *J. Organomet. Chem.* **1996**, 514, 163.
- [13] C. Castellani, S. Ottani, *Acta Crystallogr., Sect. C* **1997**, 53, 794; D. Kovala-Demertzi, D. Mentzafos, A. Terzis, *Polyhedron* **1993**, 11, 1361.
- [14] a) H. M. Krishna Murthy, T. N. Bhat, M. Vijayan, *Acta Crystallogr., Sect. B* **1981**, 37, 1102; b) H. M. Krishna Murthy, M. Vijayan, *Acta Crystallogr., Sect. B* **1979**, 35, 262.
- [15] a) K. V. Andersen, S. Larsen, B. Alhede, N. Gelting, O. Buchardt, *J. Chem. Soc., Perkin Trans. 2* **1989**, 1443; b) M. Krishna Murthy, T. N. Bhat, M. Vijayan, *Acta Crystallogr., Sect. B* **1983**, 39, 315.
- [16] K. C. Molloy, T. G. Purcell, K. Quill, I. W. Nowell, *J. Organomet. Chem.* **1984**, 267; A. R. Forrester, S. J. Garden, R. A. Howie, J. L. Wardell, *J. Chem. Soc., Dalton Trans.* **1992**, 2615.
- [17] A. Addison, R. T. Nageswara, J. Reedijk, J. Van Rijn, G. C. Verschoor, *J. Chem. Soc., Dalton Trans.* **1984**, 1349.
- [18] E. R. T. Tiekink, *Appl. Organomet. Chem.* **1991**, 5, 1; E. R. T. Tiekink, *Trends Organomet. Chem.* **1994**, 1, 71.
- [19] R. R. Holmes, R. O. Day, J. F. Vollano, J. M. Holmes, *Inorg. Chem.* **1986**, 25, 2490; R. G. Vollano, R. O. Day, D. N. Rau, V. Chandrasekhar, R. R. Holmes, *Inorg. Chem.* **1984**, 23, 3153.
- [20] V. Chandrasekhar, R. O. Day, R. R. Holmes, *Inorg. Chem.* **1985**, 24, 1970; R. R. Holmes, C. G. Schmid, V. Chandrasekhar, R. O. Day, J. M. Holmes, *J. Am. Chem. Soc.* **1987**, 109, 1408; R. G. Swisher, J. F. Vollano, V. Chandrasekhar, R. O. Day, R. R. Holmes, *Inorg. Chem.* **1984**, 23, 3147.
- [21] K. C. Molloy, S. J. Blunden, R. Hill, *J. Chem. Soc., Dalton Trans.* **1988**, 2495.
- [22] K. Nakamoto, 'Infrared and Raman Spectra of Inorganic and Coordination Compounds', 4th edn., J. Wiley & Sons, New York, 1986.
- [23] A. Galani, M. A. Demertzis, M. Kubicki, D. Kovala-Demertzi, *Eur. J. Inorg. Chem.* **2003**, 9, 1761.
- [24] teXsan for Windows, version 1.06, Crystal Structure Analysis Package, *Molecular Structure Corporation*, 1997–1999.
- [25] G. M. Sheldrick, SHELXL97, program for crystal-structure refinement, University of Göttingen, 1997.

Received March 11, 2004